



DOI: 10.58224/2618-7183-2026-9-1-1



Assessment of seismic response of a 29-storey building on raft and piled raft foundations considering soil–structure interaction

Pshenichkina V.A.¹ , Ivanov S.Yu.^{1,*} , Drozdov V.V.¹ ,
Sabitov L.S.² , Kiiamova L.I.² 

¹ Volgograd State Technical University, Russia,
² Moscow State University of Civil Engineering, Russia

Abstract: This paper presents a comparative analysis of the performance of raft and piled raft foundations using the case study of a 29-storey building designed for the seismically hazardous area of Grozny. The investigation is based on numerical modelling of the interaction within the “structure–foundation–multilayered soil” system taking into account the actual geotechnical conditions and dynamic properties of soil. Seismic loading is considered as a stationary random process. The analysis investigates the distribution of resonant frequencies of the system, the spectral density of the random acceleration function of the system, and its dynamic amplification factor. Frequency characteristics of the building were obtained using the LIRA-SOFT software package. The evaluation of the dynamic amplification factor was carried out by solving a stochastic problem of wave propagation in a multilayered medium.

The results demonstrate that the piled raft foundation reduces the dynamic response of the building. Despite its higher cost, the use of such a foundation is justified in the conditions of increased seismic hazard and weak soils. The obtained findings allow us to recommend a piled raft foundation as the preferred structural solution for high-rise buildings under engineering-geological and seismic conditions similar to those of Grozny.

Keywords: earthquake-resistant buildings, dynamic amplification factor, amplitude-frequency response, resonant frequencies, “structure–foundation–multilayered soil” system, piled raft foundation, raft foundation, probabilistic analysis

Please cite this article as: Pshenichkina V.A., Ivanov S.Yu., Drozdov V.V., Sabitov L.S., Kiiamova L.I. Assessment of seismic response of a 29-storey building on raft and piled raft foundations considering soil–structure interaction. *Construction Materials and Products*. 2026. 9 (1). 1. DOI: 10.58224/2618-7183-2026-9-1-1

*Corresponding author E-mail: stassuz-1-14@yandex.ru

1. INTRODUCTION

The current RF Construction Regulations (SP 14.13330.2018) recommend that foundations of tall earthquake-resistant buildings on non-rocky soils should be executed as pile, piled raft, or solid slab raft foundations. In engineering practice, the most common solutions are raft foundations and piled raft foundations. The former ensure high overall spatial stiffness, while the latter provide efficient transfer of loads to deeper dense soil layers. However, no unified approach has yet been developed for selecting the optimal foundation type in seismically hazardous areas.

A number of researchers emphasize the cost-effectiveness of raft foundations, noting their sufficient bearing capacity even for high-rise buildings. For instance, study [1] presents the analysis results for a 21-storey reinforced concrete frame building located on soils composed of a sand–silt–clay mixture with satisfactory bearing capacity. The building is designed in Seismic Zone III (Lucknow, India). It was established that the raft foundation carried higher loads as compared to isolated, strip, or combined foundations, while being significantly less expensive than the pile foundation.

At the same time, other studies highlight the insufficient punching shear resistance of raft foundations under seismic load [2]. For a 20-storey reinforced concrete frame building, the performance of three foundation types – raft, pile, and piled raft ones – was analyzed at various values of soil bearing capacity, pile thickness, diameter, and length. Based on the combined criteria of settlement, punching shear resistance, and soil stresses, the piled raft foundation was recognized as safe, whereas the raft and pile foundations failed to meet at least one of the verification requirements.

The choice of foundation should be based on site-specific geotechnical conditions and the level of seismic risk. Pile foundations are advisable where upper soil layers are weak or susceptible to liquefaction, but they require careful consideration of kinematic and inertial effects, especially in stratified soils.

Research [3] shows that a piled raft foundation can reduce settlements by up to 51% and decrease pressure on soft soils by 32–67% as compared to other foundation types, thus ensuring higher seismic resistance. The authors stress the necessity of integrated modelling of the “structure–foundation–soil” system for a correct assessment of dynamic response, since separate modelling does not reflect the actual interaction and may lead to erroneous engineering decisions. This conclusion is supported by several other works [4–8].

Research [9] indicates that a raft foundation can be effective if the soil base is preliminarily improved using deep soil-cement stabilization. A comparative analysis of earthquake resistance of a 9-storey reinforced concrete frame building at a design seismicity of 8 points showed that horizontal displacements were 29.6 mm on a pile foundation and 24.3 mm on a raft foundation with improved soil.

Numerical 3D modelling of a 15-storey reinforced concrete frame building with four foundation alternatives (rigidly fixed soil, shallow foundation, piled raft, and pile foundation with floating piles) in soft homogeneous soil [10,11], as well as a 12-metre high four-storey frame structure with three foundation alternatives (natural soil, floating piles, and end-bearing piles) in soils consisting of three engineering-geological elements [12] demonstrated that natural soil properties and foundation type significantly affect the seismic response of buildings, altering the dynamic characteristics of the “structure–foundation–soil” system.

The choice of foundation remains to be a critical issue in earthquake-resistant construction, particularly under complex geotechnical conditions. Analysis of seismic free-surface response during the propagation of a shear wave through randomly heterogeneous layered soils shows a significant deviation from the idealized homogeneous model [13]. Stochastic heterogeneity

increases damping and shifts the frequency response of the soil base – toward lower frequencies for homogeneous models, and toward higher frequencies with amplified response for randomly layered soils, especially in the presence of soft interlayers [14, 15].

As shown in [16, 17], reliable modelling of soil–structure interaction requires considering spatial heterogeneity, uncertainty of soil parameters, and nonlinear soil behavior under seismic excitation. The critical parameters include shear modulus and internal damping ratio.

The dynamic response of a structure is primarily governed by resonant phenomena induced by seismic wave propagation and depends on the correlation of stiffnesses of the heterogeneous soil base, the foundation, and the superstructure, as well as on the frequency content and duration of the earthquake [18, 19]. Resonant characteristics of the “structure–foundation–soil” system are strongly affected by the sequence and thickness of soil layers with different wave properties and by the statistical variability of their parameters [20]. Stress state in the foundation soil, including contact pressures beneath the foundation, should also be taken into account.

The objective of this study is to perform a comparative analysis of the dynamic response of the “structure–foundation–layered soil” system and the stress state of the soil for two foundation types designed for one and the same building in Grozny. Using the model of a horizontally layered medium, the resonant characteristics of the system are determined, including amplitude-frequency response, spectral densities of accelerations of the system, and dynamic amplification factors. The comparison results provide conclusions regarding the rational application of the above foundation types with respect to soil–structure joint work under seismic load.

2. METHODS AND MATERIALS

Analytical model of the “structure–layered soil” system

The analytical model of the “structure–layered soil” system with an arbitrary number of layers is shown in Fig. 1.

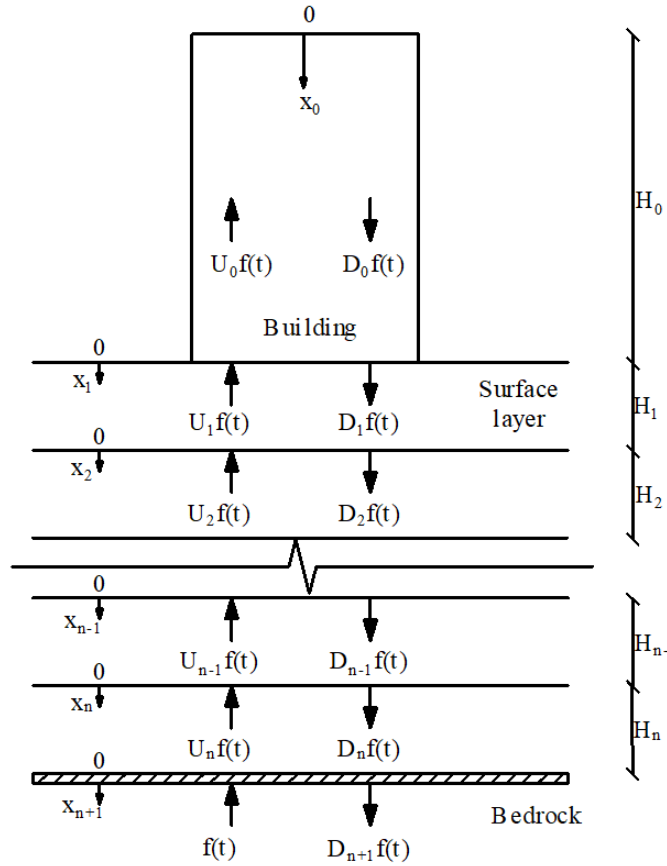


Fig. 1. Analytical model of the “structure–layered soil” system.

The bedrock is considered as a homogeneous, isotropic, elastic half-space [20]. The surface soil layer is represented as a heterogeneous stratified medium. The structure is modelled as a shear member replaced by an equivalent layer with reduced characteristics and is considered as the upper (zero) layer of the multilayer system.

Each layer is characterized by its own physical and mechanical parameters: density ρ_i , shear modulus G_i , damping decrement δ_i , shear wave velocity V_{si} , and thickness H_i .

The seismic impact is defined as a plane vertically propagating transverse shear wave $\tilde{f}(t)$ originating in the bedrock. The adopted model enables analysis of the joint wavefield in the structure and the layered soil, providing an assessment of resonant phenomena within the system.

The seismic acceleration function of the soil base $\tilde{f}(t)$ is assumed to be a stationary one with zero mathematical expectation and spectral density $S_f(\omega)$.

The probabilistic problem of vibration of the multilayered system subjected to random seismic load is solved through the method of spectral canonical representations.

The function $\tilde{f}(t)$ is expressed as:

$$\tilde{f}(t) = \sum_k \tilde{Q}_k e^{i\omega_k t} \quad (1)$$

where $\tilde{Q}_1, \tilde{Q}_2, \dots, \tilde{Q}_k$ are uncorrelated random variables. Their variances form the spectrum of the input stationary random function,

$e^{i\omega_k t}$ are deterministic input coordinate functions.

When the process represented by expansion (1) passes through a linear system, the relation between the input and output processes is described by:

$$L\tilde{F} = \tilde{f} \quad (2)$$

Then the output random process can also be expressed as:

$$\tilde{F}(t) = \sum_k \tilde{Q}_k h(i\omega_k) e^{i\omega_k t} \quad (3)$$

where $\psi_k(t) = h(i\omega_k) e^{i\omega_k t}$ are deterministic output coordinate functions determined by solving the equation:

$$L\psi_k = e^{i\omega_k t} \quad (4)$$

$h(i\omega_k)$ is the frequency characteristic of the system.

If the random function is represented in the canonical expansion form (1), its transformations reduce to the transformation of deterministic input coordinate functions (4).

The spectral density of the output random function $\tilde{F}(t)$ is determined as (5):

$$S_F(\omega) = |h(i\omega_k)|^2 \cdot S_f(\omega) \quad (5)$$

Its variance is given by (6):

$$D_F(x) = \int_0^\infty S_f(\omega) d\omega \quad (6)$$

Based on these probabilistic characteristics of the system (5,6), the dynamic amplification factor is computed as an integral indicator of the amplification of seismic response at the output (3) as compared to the impact at the input (1). Within the adopted model, it is determined as the ratio of the standard deviations of accelerations of the output and input random functions:

$$\beta(x) = \sqrt{\frac{D_F(x)}{D_{Fn+1}}} \quad (7)$$

Vibrations of the multilayered medium with damping under harmonic load of the form $e^{i\omega t}$ are described by the system of equations (8):

$$F_i(\omega, t) = U_i \cdot e^{i\omega(t + \frac{x_{i+1}}{v_i})} \cdot e^{-i c_i \cdot x} + D_i \cdot e^{i\omega(t + \frac{x_{i+1}}{v_i})} \cdot e^{-i c_i \cdot x}, \quad x_{i+1} = x_i - H_i \quad (8)$$

where $i = 0, 1, \dots, n + 1$ and by the boundary conditions:

$$G_0 \frac{\partial \tilde{F}_0(x_1, t)}{\partial x} = 0, \text{ at } x_0 = 0,$$

$$U_{n+1}(t) = e^{i\omega t}, \tilde{F}_{n+1}(x, t) = e^{i\omega t} - D_{n+1} \cdot e^{i\omega t}, \text{ at } x_n = H_n,$$

where U_i and D_i are the amplitudes of incident and transmitted waves in the layer, respectively;

$c_i = c_{1i} - i \cdot c_{2i}$, $i = 0, 1, \dots, n$ is the complex wave number.

The amplitudes $U_0(\omega), \dots, U_{n-1}(\omega), D_0(\omega), \dots, D_n(\omega)$ are determined by solving the system of linear equations $AX = B$ for each frequency value ω .

After transformations, the equations of the stationary state of the system are obtained:

$$\begin{aligned}
 F_0(\omega, x_0) &= U_0(\omega) \cdot e^{i \frac{\omega}{v_0} (x_0 - H_0 - c_{10}(\omega) \cdot x_0)} \cdot e^{-\frac{\omega}{v_0} (c_{20}(\omega) \cdot x_0)} + D_0(\omega) \cdot e^{-i \frac{\omega}{v_0} (x_0 + c_{10}(\omega) \cdot x_0)} \cdot e^{-\frac{\omega}{v_0} (c_{20}(\omega) \cdot x_0)} \\
 &\dots \\
 F_n(\omega, x_n) &= U_n(\omega) \cdot e^{i \frac{\omega}{v_n} (x_n - H_n - c_{1n}(\omega) \cdot x_n)} \cdot e^{-\frac{\omega}{v_n} (c_{2n}(\omega) \cdot x_n)} + D_n(\omega) \cdot e^{-i \frac{\omega}{v_n} (x_n + c_{1n}(\omega) \cdot x_n)} \cdot e^{-\frac{\omega}{v_n} (c_{2n}(\omega) \cdot x_n)} \\
 F_{n+1}(\omega, x_{n+1}) &= F_{n+1}(\omega, 0) = 1 + D_{n+1}(\omega) \cdot 1
 \end{aligned} \tag{9}$$

The amplitude-frequency response (AFR) of the “structure – soil” system is computed by the formula (10)

$$h(\omega, x) = \frac{F(\omega, x_i)}{F_{n+1}(\omega, 0)}, \tag{10}$$

where $x_i = 0, \dots, H_i$; $H_i = H_0 + H_1 + \dots + H_n$

$F(\omega, x)$ is the amplitude of vibrations of the entire package of layers,

$F_{n+1}(\omega, x)$ is the wave amplitude at the “surface layer – bedrock” boundary.

To compute the resonant frequencies, spectral densities, variances, dynamic amplification factors, as well as the design accelerograms for each layer and the system as a whole, the software tool developed by the authors is used [21].

3. RESULTS AND DISCUSSION

Characteristics of the Case Study Building

The object of investigation is a 29-storey building within a complex of multi-storey residential buildings with integrated non-residential premises and an underground parking facility, located in Grozny. The plan of a typical floor (12th to 20th) is shown in Fig. 2.

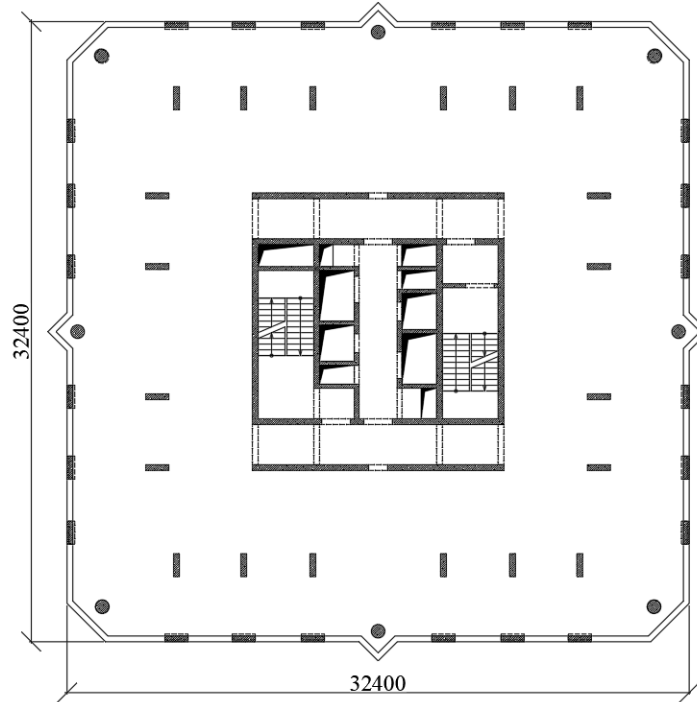


Fig. 2. Typical floor plan (12th to 20th floor).

The building parameters:

total wall area – 9807 m²; storey height - 3.1 m; slab thickness – 0.2 m; density of reinforced concrete walls and floor slabs – 2.5 t/m³; elastic modulus of reinforced concrete walls and floor slabs – 3 · 10⁶ t/m²; Poisson’s ratio – 0.2.

Total number of storeys (including the underground ones) – 32.

Taking into account that the distances between structural elements of the building (floor slabs, load-bearing walls, partitions) are significantly smaller than the seismic wavelength, the structure can be considered as a continuous medium.

The building is modelled as a shear member with equivalent parameters, the values of which are given in Table 1.

Table 1. Design parameters of the building.

Floor area, m ²	Fundamental frequency, ω, rad/s	Height h_b , m	Weighted average density ρ_b , g/cm ³	Shear wave velocity V_{sb} , m/s
95882	3.19	107	0.39	217.5

The key parameter for reducing the real building to a shear member model (layer 0) is the fundamental frequency of its free shear vibrations. This frequency is determined at the design stage using software tools or approximate methods [22]. In this investigation, the natural vibration frequencies of the building are obtained using the LIRA-SOFT software package.

The equivalent velocity of shear wave propagation in the building is calculated by the formula (11):

$$V_{sb} = \frac{2 \cdot \omega \cdot h_b}{\pi} \quad (11)$$

Characteristics of the Layered Soil Base

To illustrate the geotechnical conditions of the construction site, figure 3 shows a representative cross-section derived from boreholes No. 24-27. This section reflects typical soil stratigraphy in the area under consideration and is used as an example for the modelling of “structure–multilayered soil mass” interaction in this investigation. Within the 30-metre depth of geo-lithological section, 10 engineering-geological elements (EGE) are identified (Table 2).

Table 2. Engineering–geological elements (EGE) of construction site.

EGE	Layer	Description according to the nomenclature (RF National State Standard GOST 25100-2020)	Seismic category of soil
1	1	Stiff heavy silty loam, slightly collapsible, non-swelling, non-saline, mineral	II
2	2	Fine sand, medium saturation, medium density, heterogeneous, non-saline, mineral	III
3	3	Pebble gravel soil with up to 30% of semi-solid loamy aggregate, medium saturation, heterogeneous, moderately weathered, medium strength, non-saline, mineral	II
4	4,7	Pebble gravel soil with up to 30% of soft-plastic loamy aggregate, saturated, heterogeneous, moderately weathered, medium strength, mineral	II
5	5,10	Heavy soft-plastic silty loam, non-collapsible, non-swelling, mineral	III
6	6	Fine saturated sand, medium density, heterogeneous, mineral	III
7	8	Plastic sandy loam, non-collapsible, non-swelling, mineral	III
8	9	Gravelly soil with up to 40% of soft-plastic loamy aggregate, saturated, heterogeneous, moderately weathered, medium strength, mineral	II

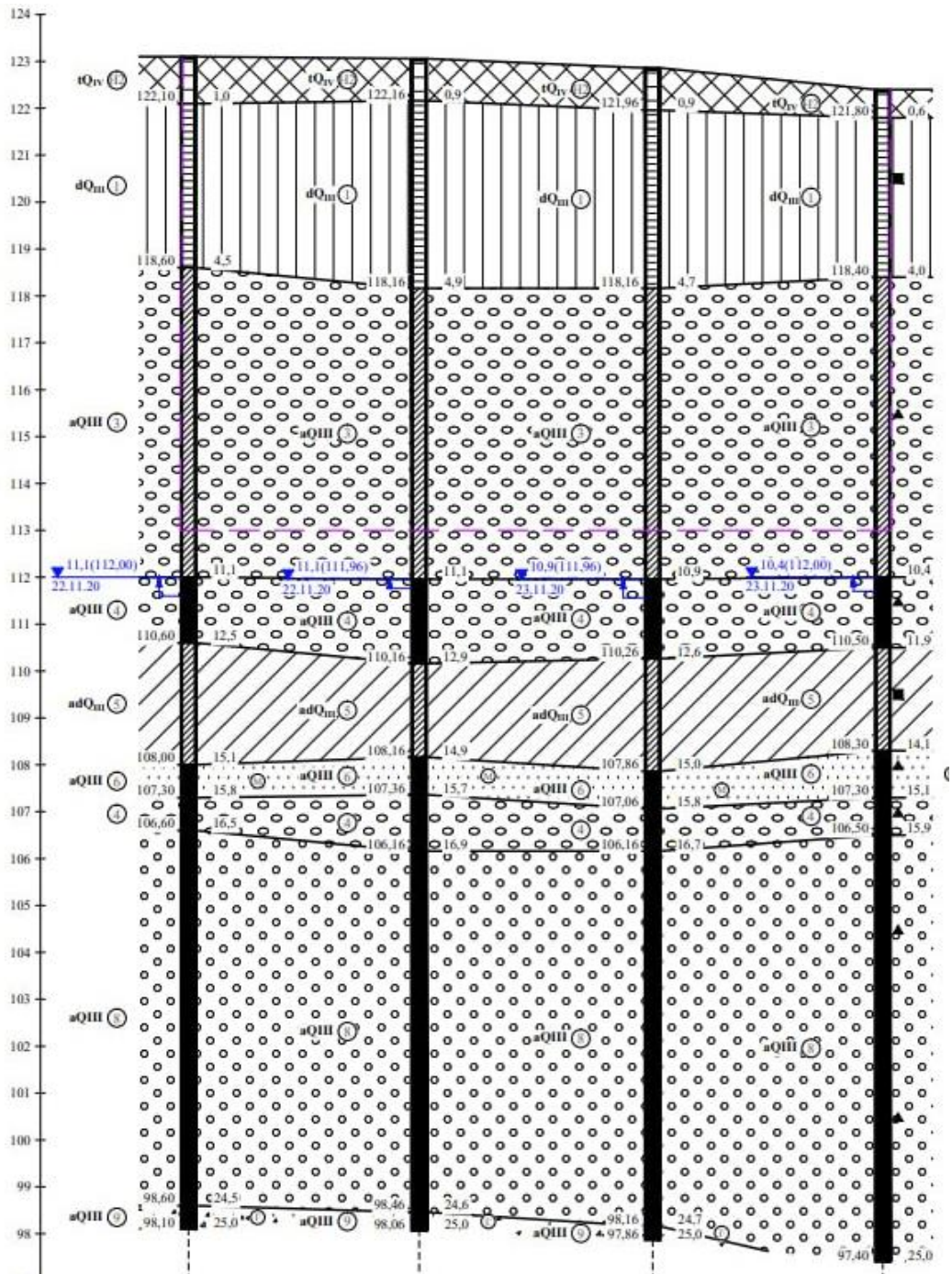


Fig. 3. Engineering–geological cross-section of the site.

Seismicity of the site is 7.99 points on the MSK-64 scale, with maximum acceleration values of 0.223 g for the horizontal component and 0.133 g for the vertical component. At the foundation pit bottom, seismicity is assessed at 8.0 points, with maximum acceleration values of 0.223 g for the horizontal component and 0.133 g for the vertical component. According to the field surveying of engineering–geological conditions, the construction site soils belong to categories II and III by seismic properties. The design soil mass is classified as category III.

From borehole and geophysical survey data, soil layer thicknesses and lithology as well as the weighted average wave velocities were determined (Fig. 4).

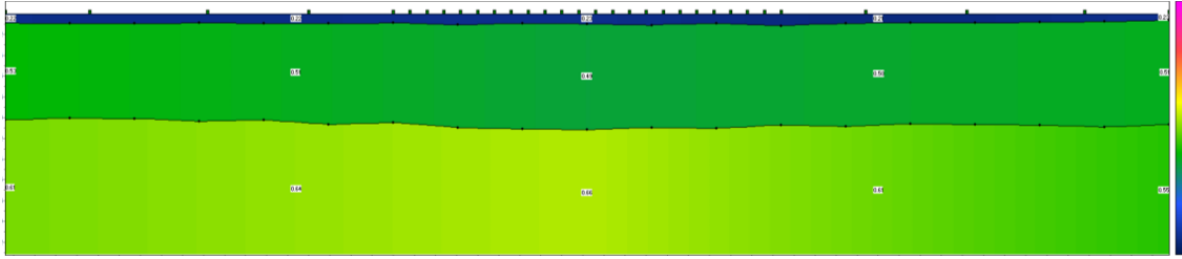


Fig. 4. Velocity profile.

The design parameters of the layered soil medium are given in Table 3.

Table 3. Parameters of layers of the geological profile.

Layer	Lithology	H_i, m	H, m	$V_p, \text{m/s}$	$V_s, \text{m/s}$	$\rho_i, \text{g/cm}^3$
1	EGE-2	1.2	1.2	420.0	230.0	1.79
2	EGE-3+4+5+6	8.9	10.1	910.0	490.0	2.10
3	EGE-4+8+5+9+10	19.9	30.0	2170.0	680.0	2.08

The following designations are used in the table: H_i – layer thickness, H – depth of the layer location, V_p – compressional wave velocity in the layer, V_s – shear wave velocity in the layer, ρ_i – layer density.

Synthesized accelerograms of heavy earthquakes recommended by the Schmidt Institute of Physics of the Earth of the Russian Academy of Sciences were used for mathematical modelling of strong-motion soil responses (access at <http://seismorus.ru>). Three-component accelerograms (for horizontal X and Y components, and for vertical Z component) corresponding to soils of seismic category III were applied.

Numerical modeling of soil response to heavy earthquakes was performed using the NERA software, which implements a modified SHAKE-91 algorithm to analyze response spectra of various types of soil.

Fig. 5 shows the design accelerograms at free soil surface, and Fig. 6 presents the envelope of dynamic amplification factors.

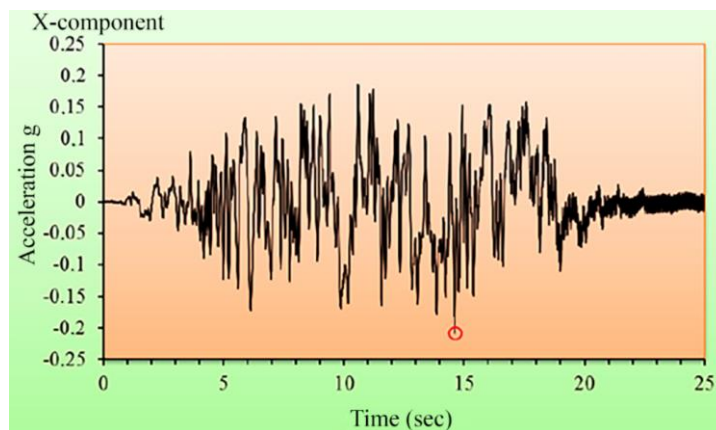


Fig. 5. Design accelerograms for the horizontal X-component at free soil surface.

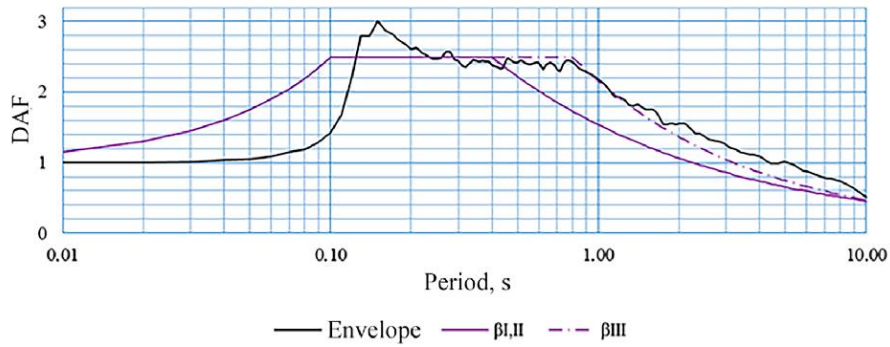


Fig. 6. Diagram of dynamic amplification factor (envelope) compared to the reference values for soils of seismic category III according to the RF Construction Regulations SP 14.13330.2018.

Using the authors’ software [21], the dynamic amplification factor was determined for a three-layer soil profile of the construction site with weighted average wave velocities (Fig. 7). Each layer was assigned its physical-mechanical characteristics: density, shear modulus, shear wave velocity, damping decrement, and thickness (Table 4).

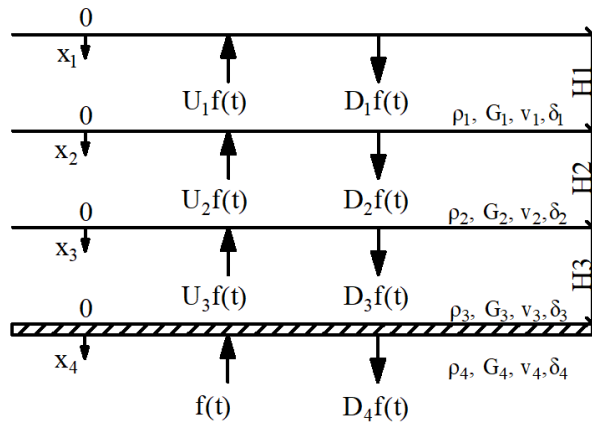


Fig. 7. Analytical model of the soil base.

Table 4. Design parameters of soil layers at the construction site.

Soil layers according to the geological profile	Thickness of layer H_i , m	Shear wave velocity V_{Si} , m/s	Density of layer ρ_i , g/cm ³	Damping decrement δ_i
Layer 1	1.2	230	1.79	0.8
Layer 2	8.9	490	2.1	0.8
Layer 3	19.9	680	2.08	0.8

The resonant frequency spectrum of the multilayer system includes the natural frequencies of all the constituent layers. It is worth noting that within the system, these frequencies differ from the natural frequencies of the layers when they are considered as individual homogeneous media.

According to the analysis results, the predominant vibration period of the three-layer soil system under consideration is $T_1 = 0.163$ s. It coincides with the first vibration period of the third layer taken as an element of the system. That is, the resonant period at the construction site under analysis in the range of [0,10 s] is determined by the physical and mechanical characteristics of the third layer. Accordingly, the first resonant frequency is $\omega_1 = 38.6$ s⁻¹.

The graph of the dynamic amplification factor for the 30-metre deep soil section is shown in Fig. 8.

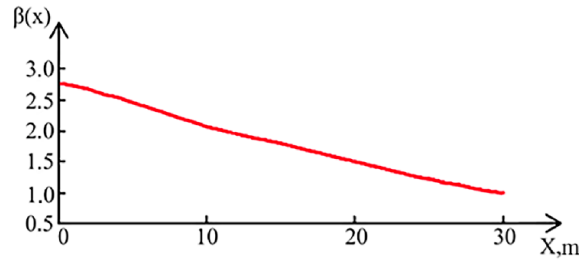


Fig. 8. Dynamic amplification factor graph.

The dynamic amplification factor at free surface is $\beta = 2.82$, and it is $\beta = 3.05$ according to field seismological measurements. The discrepancy amounts to 7.5%.

At the same time, when the response from the structure is not taken into account, the parameters of seismic load at the free surface of the soil base do not allow an objective picture of resonant phenomena in the “structure – soil” system. The resonant frequency spectrum of the system also depends on the chosen type of foundation.

Subsequently, using the software [21], we perform an assessment of the building’s dynamic characteristics for two foundation types – a raft foundation and a piled raft foundation – taking into account the interaction with the heterogeneous layered soil base.

Calculation of the Dynamic Characteristics of the Building on a Raft Foundation

Fig. 9 shows the analytical dynamic model of the building on a raft foundation. The embedment depth of the foundation is 8.4 m. The raft slab is considered as a perfectly rigid body with homogeneous physical–mechanical properties. The shear wave velocity in the raft slab is determined as:

$$V_{\phi} = \sqrt{\frac{G}{\rho}} = 2236 \text{ m/s}, \tag{12}$$

where:

G – shear modulus, ρ – density of concrete.

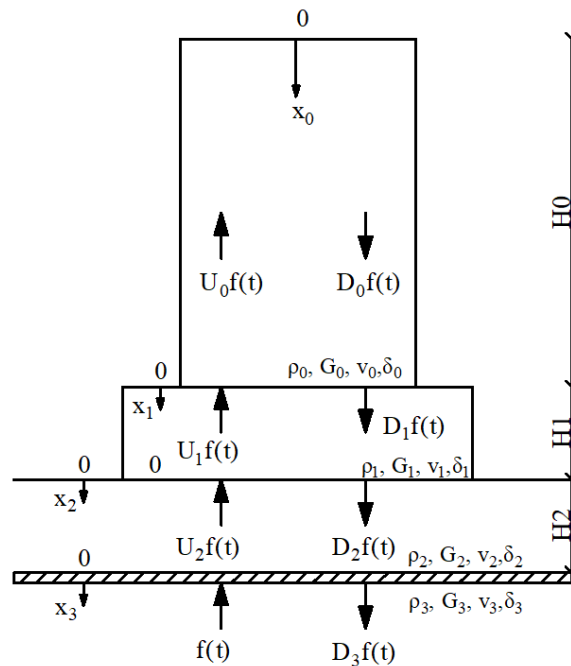


Fig. 9. Model of the “structure–raft slab–layered soil” system.

The design parameters of the layers of the “structure–raft slab–soil” system are given in Table 5.

Table 5. Design parameters of the “structure – raft slab– soil” system.

Layers of the system	Thickness of layer H_i , m	Shear wave velocity V_{Si} , m/s	Density of layer ρ_i , g/cm ³
Building	107	217.5	0.39
Raft slab	1.6	2236	2.5
Soil layer	20	680	2.08

The fundamental frequency of the spectral density of soil seismic acceleration $S_f(\omega)$ is equal to $\omega_\beta = 13,0 \text{ s}^{-1}$.

As a result of the numerical modelling, the following values of the dynamic amplification factor are obtained: $\beta_h = 6.29$ at the roof level of the building, $\beta_0 = 1.05$ at the bottom of the raft slab foundation, and the relative dynamic amplification factor is $\beta = 5.24$ (Fig. 10).

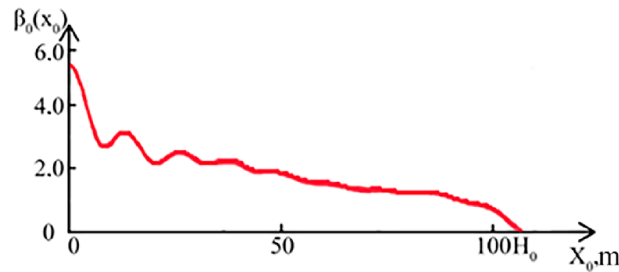


Fig. 10. Distribution of the relative dynamic amplification factor along the building height for the raft foundation case.

Calculation of the Dynamic Characteristics of the Building on a Piled Raft Foundation

Fig. 11 shows the analytical dynamic model of the building on a piled raft foundation. For modelling the dynamic interaction of the “structure–soil” system, it is represented as a layered medium, where each layer corresponds to a particular structural element or soil parcel:

- Layer 0 corresponds to the superstructure of the building;
- Layer 1 represents the slab of the raft pile cap considered as a continuous rigid medium;
- Layer 2 models a part of the pile field up to the height h_d , above which, according to the RF Construction Regulations SP 24.13330, the joint work of piles and surrounding soil is not taken into account;
- Layer 3 represents the pile–soil mass where the joint work of piles and soil occurs, with side resistance and material interaction taken into account;
- Layer 4 is the soil mass;
- Layer 5 is the soil layer conventionally assumed as bedrock.

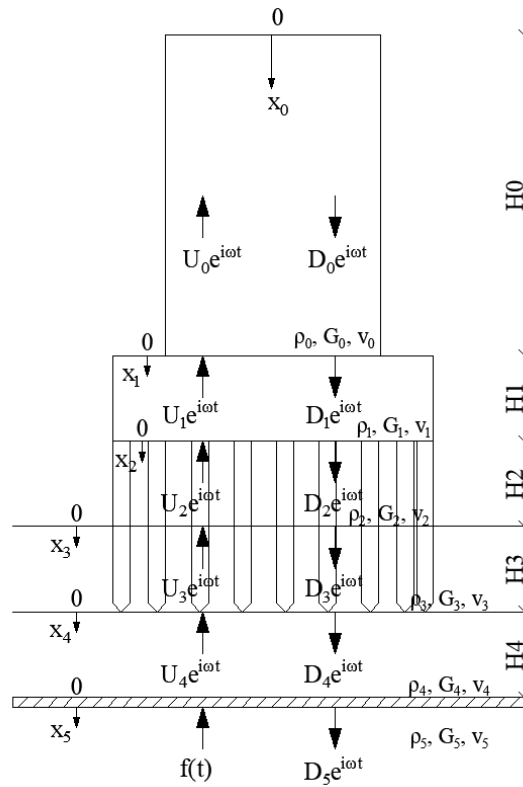


Fig. 11. Model of “structure – piled raft foundation – layered soil” system.

The wave velocity in the slab of the raft pile cap is determined according to formula (12):
 $V_p = 2236$ m/s.

According to the RF Construction Regulations SP 24.13330, the height h_d is calculated as (13):

$$h_d = \frac{\alpha_1(H + \alpha_\varepsilon \cdot \alpha_3 \cdot M)}{b_p \cdot \left(\frac{\alpha_2}{\alpha_\varepsilon} \cdot \gamma_1 \cdot \text{tg}(\varphi_1) + c_1 \right)} \quad (13)$$

where $\alpha_1, \alpha_2, \alpha_3$ are dimensionless coefficients equal to 1.2; 1.2 and 0 for rigidly fixed pile embedment into a low raft pile cap, $\alpha_\varepsilon = 0.4506 \text{ m}^{-1}$ is deformation coefficient, $b_p = 1.445$ m is conditional pile width, $\varphi_1 = 16^\circ$ is the design value of the internal friction angle of soil, $c_1 = 17$ kPa is the design value of specific soil cohesion.

Since in Layer 2 (corresponding to height h_d) the pile field does not form a continuous medium, an approximate model is applied for the analysis of dynamic characteristics in this zone. The pile field is reduced to an equivalent homogeneous cantilever bar with averaged stiffness and mass parameters (Fig. 12) reflecting the overall behavior of all the piles within the considered zone. The fundamental frequency of the equivalent cantilever bar with rigid fixed support is determined, and the equivalent wave velocity in the layer is calculated according to formula (4).

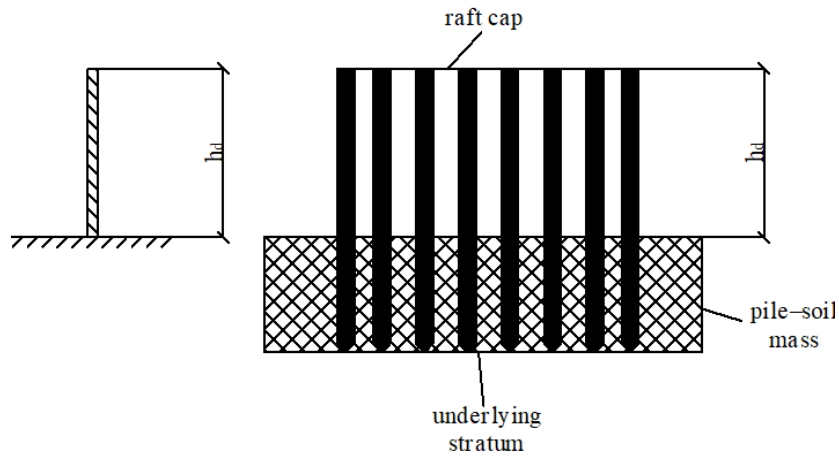


Fig. 12. Scheme of the pile field reduction to a cantilever bar.

The cross-section of the equivalent bar obtained from the reduction of the pile field within Layer 2 corresponds to the pile arrangement plan and is shown in Fig. 13.

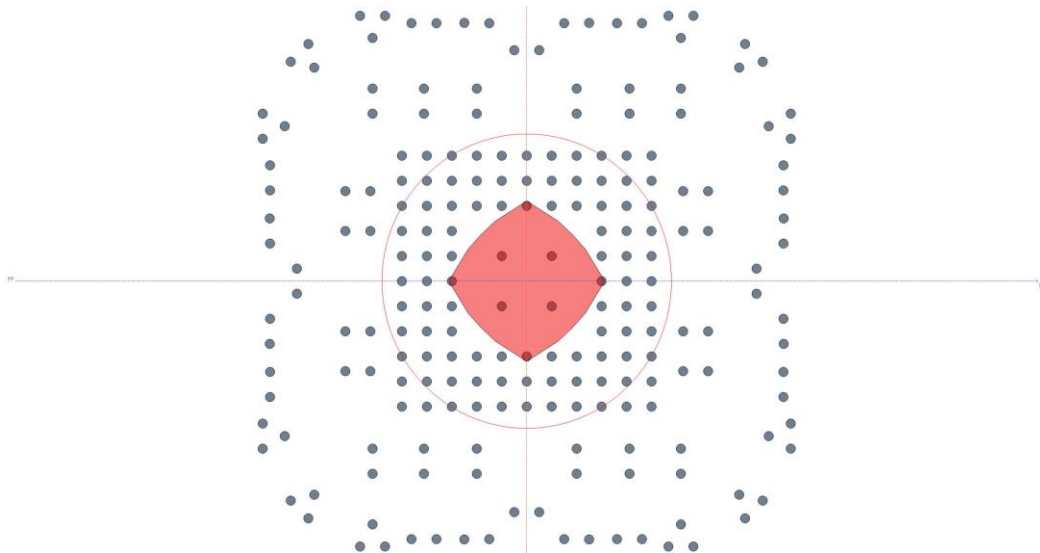


Fig. 13. Cross-section of the equivalent bar.

The fundamental frequency of the equivalent bar is calculated using the classical Euler–Bernoulli theory for flexural vibrations (14):

$$\omega_1 = \frac{1.875^2}{L^2} \cdot \sqrt{\frac{EI}{\mu}} \quad (14)$$

where:

L is bar length; I is axial moment of inertia of the bar; $\mu = \rho \cdot A$ is specific bar mass; 1.875 is characteristic root for the fundamental frequency of vibration.

For the section shown in figure 14, $I = 6516.177 \text{ m}^4$.

The fundamental frequency of the bar is $\omega_1 = 70.73 \text{ Hz}$, or 444.23 s^{-1} .

The third layer – the pile–soil mass – is considered as a continuous medium with reduced characteristics, the parameters of which are summarized below:

Pile cross-sectional area – 269.14 m^2

Soil area – 1010.86 m²
 Elastic modulus of piles – 3*10⁶ t/m²
 Shear modulus of piles – 1.25*10⁶ t/m²
 Shear modulus of soil – 0.962*10⁶ t/m²
 Shear modulus of pile–soil mass – 1.023*10⁶ t/m²
 The characteristics of all the layers are given in Table 6.

Table 6. Design characteristics of the layers.

Layers of the system	Thickness of layer H _i , m	Shear wave velocity V _{Si} , m/s	Density of layer ρ _i , g/cm ³
Building	107	217.5	0.39
Raft slab	1.6	2236	2.5
Pile field	6.53	1846	0.53
Pile–soil mass	6.47	2172.24	2.168
Soil layer	7	680	2.08

The values of the dynamic amplification factors are obtained at the building roof level β_h = 4.63, at the top surface of the slab of raft pile cap β₀ = 0.77, and the relative dynamic amplification factor is β = 3.86 (Fig. 14).

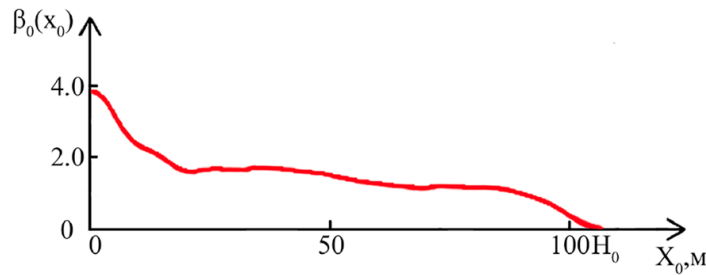


Fig. 14. Distribution of the relative dynamic amplification factor along the building height for the case of piled foundation with raft pile cap.

Thus, the dynamic amplification factor of the “structure–soil” system is 5.24 for the raft foundation case, whereas it is 3.86 for the piled raft foundation case.

Values of dynamic amplification factors comparable to those obtained in this investigation were also reported in [23].

For the system with a raft foundation, the power spectral density $S_F(\omega)$ of the output random acceleration function at the top of the raft slab has two maxima – at frequencies $\omega_1 = 16.0 \text{ s}^{-1}$ and $\omega_2 = 52.0 \text{ s}^{-1}$ in the range of fundamental frequencies of seismic impact $[0,60] \text{ s}^{-1}$. The first one corresponds to the second natural flexural frequency of the building (14.2 s^{-1}), the second one corresponds to the first vibration frequency of soil Layer 3. For the system with a piled raft foundation, the output spectral density at the top of the raft slab has one maximum at frequency $\omega_1 = 13.8 \text{ s}^{-1}$. In other words, seismic load of the building with a raft foundation is formed by the vibrations of both the building itself and the lowest soil layer. For the piled raft foundation case, the dynamic amplification factor is determined only by the resonant frequencies of the building. The stiffness of the pile cap slab, the pile field, and the pile–soil mass shifts the resonant frequency of soil Layer 3 toward higher values ($\omega_2 = 76.4 \text{ s}^{-1}$), thereby reducing the influence of the soil on the vibrations of the entire system and consequently lowering seismic load on the building.

4. CONCLUSIONS

This study presents a comprehensive numerical investigation of the “structure–foundation–soil” system for two types of foundations: a raft foundation and a piled raft foundation. The object of modelling is a 29-storey building under design for the seismically hazardous area of Grozny.

The analysis of the system’s dynamic response showed that the use of a piled raft foundation leads to a reduction in the dynamic amplification factor as compared to a raft foundation. For a flexible building, the relative dynamic amplification factor was 5.24 for a raft foundation, whereas it was 3.86 for a piled raft foundation. Similar patterns are observed for buildings of medium and high stiffness, where a reduction in dynamic response is also observed when a piled raft foundation is applied. It was established that with growing stiffness of the superstructure, the dynamic amplification factor decreases while the natural frequencies of the system increase, thus confirming a reduced sensitivity of the building to seismic impact.

Given the geotechnical and seismic parameters of the project, the combined analysis of dynamic response and stress state of the soil base demonstrates that a piled raft foundation is the preferable solution. It provides a reduction in the system’s dynamic response, ensures the stability of the stress state in the foundation soil, and complies with safety requirements of construction regulations.

REFERENCES

1. Kumar A., Kulbhushan K.K. Design of earthquake resistant structure of multi-story RCC building. *International Research Journal of Engineering and Technology*. 2019. 6 (6). P. 89 – 94.
2. Dhage A., Solanke S.S. Comparative analysis of raft, pile and piled raft foundation using designing software. *IOP Conference Series: Earth and Environmental Science*. 2023. 1193 (1). P. 1 – 8. DOI: 10.1088/1755-1315/1193/1/012006.
3. Waghela B.R., Velakkappadi D.D., Yadav P.P., Mohammad Naved Q. Comparison of building with and without foundation resting on soft soil. *International Journal for Research Trends and Innovation*. 2023. 8 (4). P. 1480 – 1486.
4. Bapir B., Abrahamczyk L., Wichtmann T., Prada-Sarmiento L.F. Soil-structure interaction: A state-of-the-art review of modeling techniques and studies on seismic response of building structures. *Frontiers in Built Environment*. 2023. 9. P. 1120351. DOI: 10.3389/fbuil.2023.1120351.
5. Nguyen N.T., Ngo V.-L. A review of soil–foundation–structure interaction and structure–soil–structure interaction effects based on numerical simulations. *Journal of Water and Land Development*. 2025. 66. P. 1 – 12. DOI: 10.24425/jwld.2025.155295.
6. Jang H., Yoon J., Cho W., Lee J. Effects of structural dynamic characteristics on soil–structure interaction (SSI) analysis of high-frequency-dominant seismic excitation. *Applied Sciences*. 2025. 15 (7). P. 3679. DOI: 10.3390/app15073679.
7. Çetindemir O. A review of modeling issues on the seismic soil-pile-structure interaction. *KSCE Journal of Civil Engineering*. 2024. 28 (8). P. 3359 – 3377. DOI: 10.1007/s12205-024-1108-2.
8. Bariker P., Kolathayar S. Dynamic soil structure interaction of a high-rise building resting over a finned pile mat. *Infrastructures*. 2022. 7. P. 142. DOI: 10.3390/infrastructures7100142.
9. Sobolev E.S., Berezin E.K., Kechina T.V. Comparative analysis of the dynamic stability of a multistorey building with different base arrangements. *Journal of Physics: Conference Series*. 2021. 1928 (1). P. 012018. DOI: 10.1088/1742-6596/1928/1/012018.
10. Klyuev S.V., Slobodchikova N.A., Saidumov M.S., Abumuslimov A.S., Mezhidov D.A., Khezhev T.A. Application of ash and slag waste from coal combustion in the construction of the earth bed of roads. *Construction Materials and Products*. 2024. 7 (6). P. 3. DOI: 10.58224/2618-7183-2024-7-6-3.

11. Hokmabadi A.S., Fatahi B. Influence of foundation type on seismic performance of buildings considering soil–structure interaction. *International Journal of Structural Stability and Dynamics*. 2016. 16 (12). P. 1550043. DOI: 10.1142/S0219455415500431.
12. Zubritsky M.A., Ushakov O.Yu., Sabitov L.S., Alekhin V.N. Foundation type influence on the construction site seismicity. *Akademicheskij Vestnik UralNIIproekt RAASN*. 2024. 2. P. 70 – 74.
13. Messaoudi A., Nourredine M., Hadid M., Laouami N. Effects of soil heterogeneities on its seismic responses. *Proceedings of the 7th International Conference on Earthquake Engineering and Seismology*. 2024. P. 221 – 232. DOI: 10.1007/978-3-031-57357-6_19.
14. Messaoudi A., Mezouar N., Hadid M., Laouami N. Effects of soil heterogeneities on its seismic responses. *Lecture Notes in Civil Engineering*. 2024. 401. P. 221 – 232. DOI: 10.1007/978-3-031-57357-6_19.
15. Berkane D., Harichane Z., Guellil M.E. et al. Investigation of soil layers stochasticity effects on the spatially varying seismic response spectra. *Indian Geotechnical Journal*. 2019. 49. P. 151 – 160. DOI: 10.1007/s40098-018-0301-y
16. Guellil M.E., Harichane Z., Çelebi A. Comparison between non-linear and stochastic methods for dynamic SSI problems. *Advances in Science, Technology and Innovation*. 2019. P. 191 – 194. DOI: 10.1007/978-3-030-01656-2_43
17. Guellil M.E., Harichane Z., Çelebi E. Seismic codes based equivalent nonlinear and stochastic soil-structure interaction analysis. *Studia Geotechnica et Mechanica*. 2020. 43 (1). P. 1 – 14. DOI: 10.2478/sgem-2020-0007
18. Khachiyani E.E. *Seismic impacts and prediction of the behavior of structures*. Yerevan: Gitutyun, 2015. 555 p.
19. Pshenichkina V.A., Rekunov S.S., Ivanov S.Yu. Probabilistic analysis of dynamic characteristics of the structure – layered foundation system. *News of Higher Educational Institutions. Construction*. 2024. 8. P. 32 – 43. DOI: 10.32683/0536-1052-2024-788-8-32-43
20. Stupishin L., Mondrus V. Energy properties of symmetric deformable systems. *International Journal for Computational Civil and Structural Engineering*. 2024. 20 (1). P. 35 – 45.
21. Ivanov S.Yu., Rekunov S.S., Pshenichkina V.A., Churakov A.A., Anokhin S.V. Dynamic characteristics of a layered system. Certificate of state registration of computer program n. 2024614957. Russian Federation. 2024.
22. Korol O.A., Barabanova T.A., Abdullazianov E.U., Sabitov L.S., Ayzatullin M.M. Stress–strain state during the formation of normal cracks in three-layer bendable reinforced concrete elements under the action of longitudinal and transverse forces. *Construction Materials and Products*. 2024. 7 (1). P. 3. DOI: 10.58224/2618-7183-2024-7-1-3
23. Nuzhdin L.V., Mikhaylov V.S. Method of accounting for resonance effects in forecasting vibrations of large-size pile foundations. *News of Higher Educational Institutions. Construction*. 2025. 5. P. 82 – 95. DOI: 10.32683/0536-1052-2025-797-5-82-95

INFORMATION ABOUT THE AUTHORS

Pshenichkina V.A., e-mail: rap_hm@list.ru, ORCID ID: <https://orcid.org/0000-0001-9148-2815>; SCOPUS: www.scopus.com/authid/detail.uri?authorId=57189646401, Volgograd State Technical University, Head of the Department of Building Structures, Foundations and Reliability of Structures

Ivanov S.Yu., e-mail: stassuz_1_14@yandex.ru, ORCID ID: <https://orcid.org/0000-0003-4770-8754>, Volgograd State Technical University, Foundations and Reliability of Structures, Assistant

Drozdov V.V., e-mail: drozdov_jm@mail.ru, ORCID ID: <https://orcid.org/0009-0008-1526-7193>, SCOPUS: www.scopus.com/authid/detail.uri?authorId=57190968037, Volgograd State Technical University, Foundations and Reliability of Structures, Senior lecturer

Sabitov L.S., e-mail: l.sabitov@bk.ru, ORCID ID: <https://orcid.org/0000-0001-7381-9752>, SCOPUS: <https://www.scopus.com/authid/detail.uri?authorId=57079229700>, Moscow State University of Civil Engineering National Research University, Doctor of Technical science (Advanced Doctor), Professor of the Department of Technology and Organization of Construction Production

Kiiamova L.I., e-mail: rostehkazan@mail.ru, ORCID ID: <https://orcid.org/0000-0002-2429-4301>, SCOPUS: <https://www.scopus.com/authid/detail.uri?authorId=58500338500>, National Research Moscow State University of Civil Engineering, Department "Construction Technologies and Construction Process Management", Assistant